Vol. 07, No. 01, pp. 1 –13 (2026)
ISSN: 2709-6904

JoCEF

JOURNAL OF CIVIL ENGINEERING FRONTIERS

www.jocivilef.org

Development of Machine Learning Algorithms to Predict the Ultimate Axial Capacity of Fire Damaged Circular Columns Repaired with CFRP Composites

Muhammad Salman[1,*], Muhammad Yaqub[2], Muhammad Noman[3], Muhammad Faizan[4], Muhammad Ahmed Javaid[5], Saad Maqsood[6]

[1] *Department of Mathematics, Computer Science and Engineering, University of Quebec at Rimouski, Canada. (Muhammad.Salman@uqar.ca)*
[2] *Civil Engineering Department, University of Engineering and Technology Taxila, Pakistan (Muhammad.Yaqub@uettaxila.edu.pk)*
[3] *Civil and Coastal Engineering Department, University of Florida, Gainesville, USA. (Muhammadnoman@ufl.edu)*
[4] *Computer Engineering Department, UET Taxila, Pakistan. (muhammadfaizandev87@gmail.com)*
[5] *Capital University of Science & Technology (CUST), Islamabad, Pakistan (muhammadahmadjavaid84@gmail.com)*
[6] *North China Electric Power University, Beijing, China. (Jamalam56@gmail.com)*

Abstract

This paper presents a study that extends the application of carbon fiber reinforced polymer (CFRP) composite confinement technology to strengthen circular concrete columns damaged by fire. This study utilized data from 125 column specimens sourced from the literature. It examined ten parameters: column diameter, height, initial compressive strength of concrete, initial tensile strength of steel, longitudinal reinforcement ratio, fire temperature, exposure time, number of CFRP layers, CFRP thickness, and CFRP tensile modulus, which were used as inputs for the model. The objective was to predict the ultimate axial strength of fire-damaged circular columns repaired with CFRP composites. This study employs both multiple regression analysis and a deep neural network (DNN) to predict the structural behavior of reinforced concrete (RC) columns and accurately forecast their repaired axial capacity. The proposed deep neural network (DNN) model demonstrated a robust agreement with experimental investigations, boasting an overall correlation factor (R) of 0.99852. Deep neural networks outperformed multiple regression analysis in predicting axial strength, with predictions closely matching experimental results from previous studies. The work also presents a parametric study to examine the effect of different input parameters on the axial strength of RC columns. Parametric analysis indicates that the repaired axial strength increases with higher concrete initial compressive strength, greater CFRP thickness and tensile modulus, and more CFRP layers, whereas it decreases with higher fire temperatures, longer exposure durations, and larger column diameters.

Keywords: *Carbon Fiber Reinforced Polymer, Deep Neural Network (DNN), Heat Damaged, Circular Concrete Columns.*
Received: September 12, 2025 / Revised: November 15, 2025 / Accepted: November 18, 2025 / Online: January 01, 2026

I. INTRODUCTION

Externally bonded fiber-reinforced polymer (FRP) circumferential wraps are a preferred method for restoring or enhancing the capacity and ability to resist distortion of concrete columns. There is considerable research evidence supporting the use of FRPs in different applications. Additionally, numerous computational models exist for designing FRP strengthening techniques for both circular and rectangular concrete columns under ambient conditions [1, 2]. There is an increasing body of research [3, 4] that has examined the behavior of reinforced concrete columns enhanced with FRP wraps during fire exposure. These columns have either been exposed to elevated temperatures or have had their mechanical characteristics diminished due to thermal effects [5].

Fire is a prevalent natural phenomenon with significant potential for causing extensive damage to buildings if left uncontrolled. There has been a global increase in incidents of structures being damaged by fire, with concrete structures being particularly vulnerable due to the loss of structural integrity during and after such events [6, 7]. Owners and insurers of infrastructure aim to minimize financial losses resulting from building closures and operational disruptions by demanding reliable, cost-effective, and expedient repair techniques [8]. In response, various methods have been employed, including the use of concrete or steel jacketing for column strengthening.

ipAcademia www.ipacademia.org

doi:10.38094/jocef701121

However, contemporary practices favor fiber-reinforced polymer (FRP) due to its rapid application and lightweight nature, which has been demonstrated to strengthen and repair damaged structures effectively [9,10]. Although considerable research has been conducted on retrofitting concrete columns with FRP [11-20], limited attention has been given to fire-damaged circular concrete columns [4]. The lack of research in this specific area is primarily due to uncertainties regarding the performance of FRP in fire conditions following repair [21]. Nevertheless, it has been noted that FRP can perform well in fire conditions when appropriate fire insulation measures are applied [22-29]

Concrete structures generally show excellent resistance to fire [30] and can typically be repaired after a fire incident [31]. This is mainly due to the fact that the concrete shell has comparatively low heat conductivity. As long as it stays intact, it protects the concrete core and embedded reinforcement at relatively reduced temperatures even during extended periods of severe heating. By reducing the harmful effects of heat on the material properties of the reinforcing bars and the core concrete, this method maintains the structural stability and ensures sufficient fire resistance, provided the member has been properly constructed [32].

With progress in scientific disciplines, machine learning (ML) and artificial intelligence (AI) have advanced considerably and are now broadly utilized across multiple industries. Deep learning, in particular, has become prominent in addressing a wide range of engineering problems [33–38]. Previous studies have applied neural networks (NNs) to predict the compressive strength of FRP-confined concrete [39–42], showing the usefulness of NNs in estimating such behavior based on material and structural factors. In existing literature, NN-based modeling has been employed to predict several parameters, such as the load capacity of fiber-reinforced cement-based matrix-encased columns, fire resistance of hollow steel members filled with concrete, residual strength of High-Performance Concrete (HPC) exposed to elevated heat, and load-bearing capacity of thermally damaged concrete strengthened with Glass Fiber-Reinforced Polymer (GFRP) [43–45]. However, in the scope of this research, which investigates the impact of Carbon Fiber-Reinforced Polymer (CFRP) on fire-deteriorated circular columns, there is a clear gap in published work addressing the creation of a DNN model for this purpose. To address this gap, the present study aims to develop and validate an optimized DNN that predicts the ultimate axial strength of CFRP-repaired, fire-damaged circular concrete columns using a curated database of 125 experimental specimens and ten key input parameters. The novelty of this work lies in applying a tailored DNN architecture to a comprehensive fire-damage dataset, comparing its performance with multiple regression analysis, and coupling the model with a parametric sensitivity study to produce actionable guidance for repair design and fire-resilience assessment

II. Methodology

To establish a robust Deep Neural Network (DNN) model and a regression model for predicting the axial capacity of fire-damaged circular concrete columns repaired with Carbon Fiber Reinforced Polymer (CFRP), a comprehensive database comprising 125 specimens sourced from existing literature was compiled. The collected data were first normalized and then used for training the DNN models. Seven models in total were built with each model possessing a different neural structure based on Multilayer Feedforward Neural Networks (MLFNNs) for the prediction of axial capacity of fire-damaged concrete columns repaired with CFRP. The models were well-tested and the best one was selected with the highest accuracy of prediction. This optimum DNN model, together with regression analysis, were subsequently employed to forecast the axial capacity of the repaired columns, and the results were compared against experimental findings presented in the literature. Besides, the model was also utilized to examine the influence of various parameters such as column height, initial compressive strength of concrete, heating duration, fire exposure temperature, and number of layers of CFRP on the axial capacity of CFRP-strengthened fire-damaged circular columns. A schematic outline of the approach adopted in this research is presented in Fig. 1 to illustrate the process step by step.

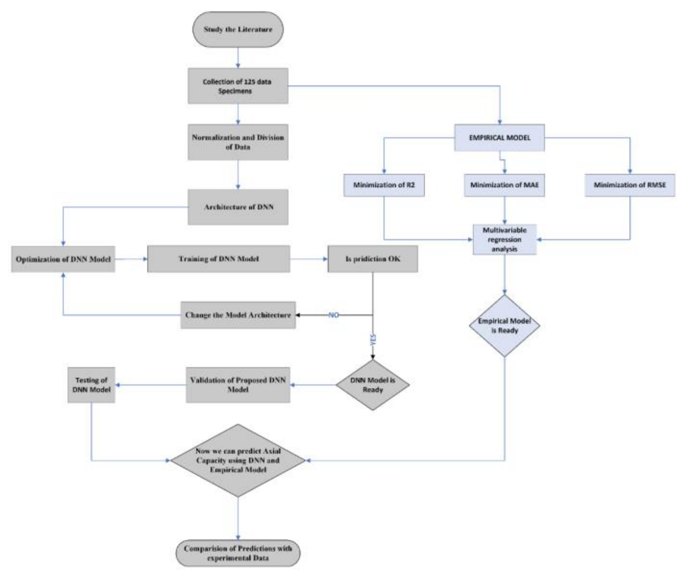

Fig. 1. The procedure of the present investigation.

2.1 *Linear regression model*

Multivariable linear regression analysis (MRA) was applied to evaluate the influence of several independent variables on the dependent variable. In this approach, the dependent variable is modeled as a linear combination of two or more predictors, as represented by the general MRA model as

$$Y=a+b_1\ X_a+b_2\ X_b+\ldots\ldots\ldots\ldots b_k\ X_k\pm e$$

In this model, Y denotes the dependent variable; a is the intercept; b_1, b_2, …, b_k represent the regression coefficients corresponding to the independent variables X_a, X_b, …, X_k; and e denotes the error term. The regression models were developed using the enter method in the Statistical Package for Social Sciences (SPSS), where all variables in a block are introduced simultaneously in a single step.

Multivariable linear regression analysis (MRA) is associated with several statistical parameters that provide insights into model performance and reliability. Among the most important are: the coefficient of determination (R^2), the correlation coefficient (R), the adjusted coefficient of determination (adjusted R^2), the standard error of the regression coefficient, the confidence level, the standard error of estimate, model error, the significance level (p-value), the t-distribution, the F-distribution, and the residuals [46, 47].

2.2: Neural Network Modelling:

2.2.1: Forward and Back propagation:

In the present study, multilayer feedforward neural networks (MLFNNs) were employed to develop models for predicting the axial capacities of CFRP-repaired, fire-damaged rectangular and square columns. Previous experiments have demonstrated that MLFNNs offer optimal estimations for FRP-wrapped sections [48, 49]. MLFNNs encompass two distinct processes: Forward Propagation. Also known as the input signal, this process involves feeding data into the neural network via input neurons in the input layer. The data is then transmitted to neurons in the first hidden layer, where each neuron computes an output based on its current weights, biases, and activation function. This information is subsequently processed in subsequent layers until it reaches the output layer, where the network generates predictions/output [50]. Backward Propagation: Following forward propagation, the network's predicted values are compared to the actual target values, and the error is determined using a loss function. The mean squared error is commonly employed as the loss function in regression applications [51]. In this research, the loss function employed during network training is represented by Equation 1. The discrepancy between the predicted and actual target values, quantified by Equation 1, serves to evaluate the network's predictive accuracy. Where T_i is the target value and O_i is the output from the DNN model.

$$Error = 1/2 \sum_{i=1}^{n} (T_i - O_i)^2 \quad (1)$$

Fig. 2 shows the processes of forward and backward propagation, offering a clear view of the neural network architecture. To reduce the error defined by the loss function, the bias values and weights of the DNN are updated through backward propagation, also known as error signal propagation. In this process, the gradient of the loss function with respect to each weight is calculated, moving in reverse from the output layer back to the input layer, based on principles of calculus [52]. After the gradients are obtained, the weights are adjusted using an optimization algorithm, most commonly gradient descent. This involves modifying the weights in the opposite direction of the gradient to reduce loss [53]. The procedure is repeated across many training cycles, allowing the weights to gradually converge. As training advances, the model becomes more effective at minimizing loss and improves its ability to make accurate predictions or classifications on new, unseen data.

2.2.2: Training & learning algorithms for DNN

The backpropagation (BP) learning method entails transmitting the input values through the network in advance, after which the difference between the estimated output and the corresponding intended output from the training dataset is calculated. This approach employs a gradient descent strategy to minimize the value of the error function. The partial derivative of the error function concerning each weight is used to determine the necessary adjustments to the network's weights and bias values for each moment. The chain rule of calculus is used to determine the BP, which is based on the gradient-descent or Jacobian technique. In many engineering applications, BP learning has replaced other methods as the standard procedure for modifying the weights and biases used in ANN training. Gradient-descent BP has three drawbacks, though: (a) it can be challenging to identify appropriate ANN topologies; (b) the multifarious error planes that are produced have several local minima, causing the BP to fall into local minimum rather than a global minimum [54-57]. An additional issue with BP training is that, due to variations in the initial weight and bias values, as well as in the data partitioning into training, validation, and test sets, an ANN may produce a different answer every time it is trained. For the same input, various ANNs trained on the same issue may produce different results. A neural network requires at least three training sessions to ensure a high level of accuracy. Twelve training algorithms in MATLAB are based on various defining criteria used to train multilayer feedforward neural networks (MLFFNNs). The gradient or Jacobian method-based training techniques are accessible through MATLAB's Neural Network Toolbox software [58, 59].

2.2.3: Activation Functions

Activation functions within a neural network play a pivotal role, imparting non-linear characteristics essential for the network to undertake complex tasks beyond linear operations. These functions determine the output of a neural network node or neuron by processing a collection of inputs and their associated weights. The network's ability to discern intricate patterns and correlations in data hinges significantly upon these activation functions [60]. The selection of an appropriate activation function has a profound impact on the efficacy and capabilities of the neural network's learning process. Previous research suggests that the choice of activation function between layers varies depending on how input parameters are processed and normalized, i.e., how they are integrated into the DNN [60]. In scenarios where identification and regression analysis problems necessitate normalizing input and output parameter values within the range of 0 to 1, the "log-sigmoid" function typically links the initial two layers (Input and hidden layers) of the DNN. In comparison, the "linear" activation function connects the last two layers (the last hidden and output layer) [61].

2.2.4: Structural Design of Neural Networks: Exploring Architectural Constructs

The neural network comprises three fundamental components: the Input layer, hidden layers, and Output layer [62]. These layers consist of interconnected cells, known as artificial neurons, which emulate the functionality of biological neurons [63]. Fig. 2 provides a concise depiction of the neural network architecture, where inputs are denoted by In1-n, hidden layer neurons by HL1-21-n, and biases by B, along with their respective neuron counts. Facilitated by the collected data, neurons within the network receive inputs from the input layer, undergo transformations within the hidden layers, and ultimately produce outputs in the output layer. Serving as conduits between layers, neurons are assigned weights, representing specific coefficients, which are then multiplied by input values. Subsequently, the resultant products are aggregated with bias values according to Equation 2. In Equation 2, the interplay between bias values and the activation function is highlighted as integral to the neural network's learning dynamics. Here, the output is determined by the activation function applied to the weighted sum of inputs, adjusted by the bias term "b." This process signifies the crucial role of bias in regulating the network's responsiveness to input signals.

$$Output = f(\sum_{i=1}^{n} (x_i \times w_i) + b) \quad (2)$$

Each input xi is multiplied by its corresponding weight wi, with the resulting products summed. The bias term, acting as an additional adjustable parameter, contributes to fine-tuning the network's responsiveness. This sum, along with the bias, is then processed through the activation function, which determines the neuron's output. This equation encapsulates the essence of neural network connectivity, illustrating how the network processes and integrates information across its layers. The operational procedures conducted within a neuron are also illustrated in Fig. 2. Specifically, Neuron HL2-1 is analyzed, elucidating the detailed processes of summation and the application of the activation function.

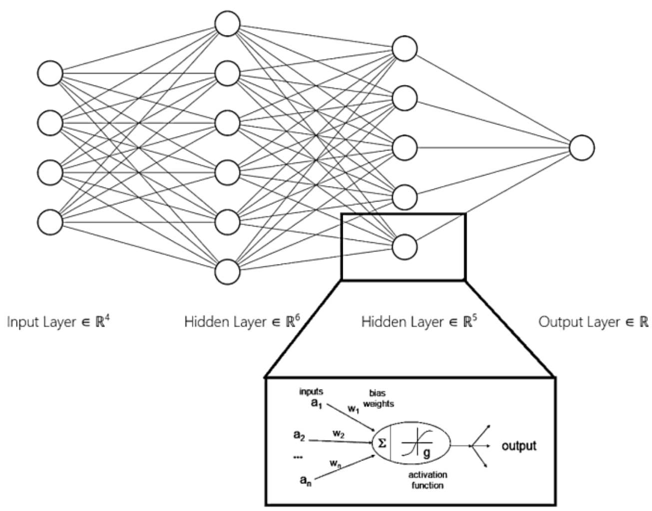

Fig. 2. Basic Architecture of Neural Network And inside processing of Neuron

III. Data Collection and Analysis:

A database comprising 125 samples was collected from various studies [5, 64-69]. Some of these studies focused solely on the confinement of circular concrete columns, serving as control specimens to investigate the effects of confinement on columns in greater detail, particularly regarding input parameters such as corner radius and number of layers. During the database development process, 10 parameters were systematically recorded from each experimental program and subsequently utilized as inputs for the neural network. These parameters encompassed the diameter of columns (mm), column height (mm), concrete's initial compressive strength (MPa), steel's initial tensile strength (MPa), longitudinal reinforcement ratio (As/Ag, %), temperature of fire (°C), fire exposure time (Mins), number of layers of CFRP (Count), thickness of CFRP (mm), and tensile E-modulus of CFRP (GPa). Additionally, the axial load capacity (in kN) of the columns was recorded as the output variable for the proposed neural network. The collected samples from various experiments are presented comprehensively in Table 1. The data obtained from the literature was divided into three distinct subsets: training, validation, and testing. Seventy percent of the collected data was allocated for training the neural networks, while the remaining 30% was divided equally into validation and testing subsets, each comprising 15% of the dataset.

TABLE I. Sample of Collected data from Literature

Column Dia (mm)	Specimen Height (mm)	Initial Compressive	Initial Tensile Strength of	As/Ag (%)	Temperature at which heated	Fire Exposed Time (min)	No of Layers of CFRP	Thickness of CFRP (mm)	Tensile modulus of CFRP (GPa)	Final Axial Capacity (kN)
200	1000	53	553	1.6	0	0	0	0	0	1439
200	1000	53	553	1.6	0	0	0	0	0	1397
200	1000	53	553	1.6	500	210	0	0	0	826
200	1000	53	553	1.6	500	210	0	0	0	946
200	1000	53	553	1.6	500	210	1	0.117	240	1356
200	1000	53	553	1.6	500	210	1	0.37	230	1701
200	1200	35	420	1.5	0	0	0	0	0	1353
200	1200	35	420	1.5	0	0	0	0	0	1351
200	1200	35	420	1.5	0	0	0	0	0	1355
200	1200	35	420	1.5	300	230	0	0	0	1196
200	1200	35	420	1.5	300	230	0	0	0	1198
200	1200	35	420	1.5	300	230	1	0.117	230	2431
200	1200	35	420	1.5	300	230	1	0.117	230	2436
200	1200	35	420	1.5	600	400	0	0	0	972
200	1200	35	420	1.5	600	400	0	0	0	977
200	1200	35	420	1.5	600	400	1	0.117	230	2160
200	1200	35	420	1.5	600	400	1	0.117	230	2163
200	1200	35	420	1.5	900	600	0	0	0	709
200	1200	35	420	1.5	900	600	0	0	0	713
200	1200	35	420	1.5	900	600	1	0.117	230	1761
200	1200	35	420	1.5	900	600	1	0.117	230	1765
370	1000	50	500	1.6	0	0	0	0	0	3957

To optimize the efficacy and performance of the training process for deep neural networks (DNNs), it is essential to normalize all variables contained within the database [60]. Following the training process, the output may be denormalized to facilitate comparative analysis. To mitigate challenges associated with low DNN learning rates [53], parameter values should be normalized within an acceptable upper and lower threshold range for each respective parameter. Thus, to refine the accuracy of estimations generated by the proposed NN model, all parameters extracted from the literature have been normalized between 0.9 and 0.2, considering variations in units. Equation 3 has been used to normalize variables pertinent to rectangular and square concrete columns.

$$\mathrm{Y} = (0.8/\Delta) \times y + (0.9 - (0.8/\Delta) \times)\mathrm{y}_{\max}) \quad (3)$$

In the normalization process, "y" represents the original value of the variable obtained from the developed dataset, while "Y" denotes the normalized value of the variable. The symbol "Δ" signifies the difference between the maximum and minimum values of the variable. For instance, in the case of the Diameter of Columns variable, the minimum value (ymin) was determined to be 150 mm, and the maximum value (ymax) was 370 mm. After normalization, the lowest value was transformed to 0.1, and the highest value became 0.9. Similarly, all other variables underwent normalization within the range of 0.1 to 0.9 before being used as inputs for model training.

3.1: Structure of Neural networks:

The architecture of DNN models plays a critical role in shaping their predictive capabilities. Determining the appropriate activation functions to be employed between each layer, as well as the total number of neurons in each layer and the overall number of hidden layers in the network, is crucial. However, due to the lack of standardized guidelines, the architecture of DNNs is tailored to the specific characteristics of the subject matter and is refined through iterative experimentation. The variables associated with each of the NN structures investigated in the present study, aimed at identifying the most efficient architecture, are detailed in Fig. 3.

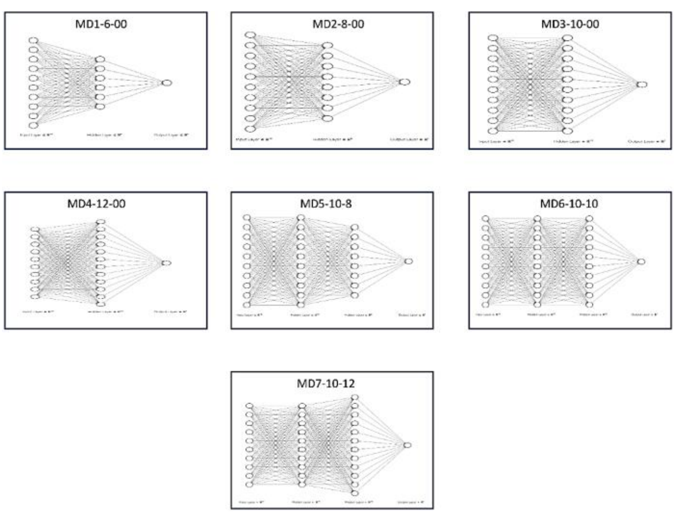

Fig. 3. Structure of proposed DNN Models

The study employed MATLAB to construct seven distinct models aimed at predicting the axial capacity of heat-damaged, CFRP-repaired circular concrete columns. Among these models, four utilized a single hidden layer (HL), while the remaining three featured double hidden layers. Activation functions were strategically chosen, with the sigmoid function employed between the input layer (IL) and the HL, as well as between the first and second HL. tanh function was applied between the output layer (OL) and last hidden layer (LHL). All of the models were trained for the number of epochs set, and this was set at 300.

One aspect of the backpropagation (BP) learning involved passing input values through the network and computing the difference between the output predicted and the target output from the training database. It employed a gradient-descent method for minimizing the error function, an inexpensive scheme to update weights and biases in neural network training in many scientific disciplines [62]. Thus, the LEARNGDM learning algorithm was applied in MATLAB for pre-training the DNNs in this study. Moreover, previous studies stressed that

second-order learning algorithms should be employed for effective and efficient training. As such, the TRAINLM algorithm, which is a member of the Newton family employing the Levenberg-Marquardt (LM) algorithm, was employed as the Training Algorithm for all the DNN models developed in this study [55, 56].

All the models consisted of ten input variables, i.e., diameter of columns (mm), column height (mm), initial compressive strength of concrete (MPa), initial tensile strength of steel (MPa), longitudinal reinforcement ratio (As/Ag %), fire temperature (°C), fire exposure duration (minutes), layers of CFRP (Count), thickness of CFRP (mm), and tensile E-modulus of CFRP (GPa). The output of every model was the axial capacity of square and rectangular concrete columns rehabilitated with CFRP following exposure to fire.

3.2: Analytical Approaches for Error Assessment:

Furthermore, this study employs three additional statistical tools Root Mean Squared Error (RMSE), Mean Squared Error (MSE), and Mean Absolute Error (MAE) to assess the performance of the DNN models. The highest value of R and the lowest values of RMSE, MSE, and MAE indicate the most optimal model. Table. 2 shows the formulas used to calculate the correlation factor (R), RMSE, MSE, and MAE, respectively.

TABLE II. DNN MODEL EVALUATION METRICS [70]

Metric	Definition	Equation
MAE	Mean absolute error	$\mathrm{MAE} = \frac{1}{n}\sum_{i=1}^{n}\lvert y_i - y'_i\rvert$
MAPE	Mean absolute percentage error	$\mathrm{MAPE} = \frac{1}{n}\sum_{i=1}^{n}\left\lvert \frac{y_i - y'_i}{y_i}\right\rvert \times 100\%$
RMSE	Root mean square error	$\mathrm{RMSE} = \sqrt{\frac{1}{n}\sum_{i=1}^{n}\left(\frac{y_i - y'_i}{y_i}\right)^2}$
R^2	Goodness of fit	$R^2 = 1 - \frac{\sum_{i=1}^{n}(y_i - y'_i)^2}{\sum_{i=1}^{n}(y_i - \overline{y})^2}$

IV. MODEL ANALYSIS

4.1 Multiple regression analysis

Regression analysis typically requires a robust relationship between the independent and dependent variables. On the other hand, when there is a significant relationship between independent variables, referred to as "multicollinearity," it can cause issues with the analysis. There is no universally recommended or universally acknowledged method for resolving the problem of multicollinearity, as it is a result of the inherent characteristics of the data. A multinomial model is created to forecast the axial capacity of a fire-damaged and CFRP-repaired circular column. In summary, the regression model can be described as follows: Table 3 presents the statistical parameters derived at the 95% confidence level, which is a regularly utilized level in statistical data analysis.

The models' validity was evaluated based on several criteria, including the behavior of the correlation coefficient (R), the T-test, the F-test, and the Durbin-Watson test. The statistical findings obtained for all models are presented in Table 3. The correlation coefficient for Model 1 is within an acceptable range, with an R value of 0.936. A high coefficient of regression does not necessarily reflect the superiority of the model. The validity of a model cannot be determined solely based on the value of R. The findings of a t-test, F-test, and Durbin–Watson test, were applied to verify consistency between the model and the experimental observations. Multiple regression analysis (MRA) was performed together with an analysis of variance (ANOVA) or the F-test. ANOVA was used to evaluate the importance of deviations from both linear and non-linear patterns in the established regression models.

TABLE III. SUMMARY STATISTICS FOR THE MODEL OF MRA (AT THE 95% CONFIDENCE LEVEL)

Dependent variable	Independent variable	Coefficient	t- Value	t- Significant	R-Value	Model error	F-Value	F- Significant	Durbin–Watson
Final Axial Capacity (kN)	(Constant)	-2208	2.50	0.01	0.967	2.56	165.9	0.000	2.452
	Column Dia (mm)	17.1	16.36	0.00					
	Column Height (mm)	-0.2	-0.65	0.51					
	Initial Compressive Strength of Concrete	35.0	7.83	0.00					
	Initial Tensile Strength of steel	-4.8	-2.12	0.03					
	As/Ag	612.2	2.41	0.01					
	Temperature at which heated	-2.5	-3.90	0.00					
	Fire Exposed Time	2.8	2.45	0.01					
	No of Layers of CFRP	177	3.28	0.00					
	Thickness of CFRP	-179.5	-0.96	0.33					
	Tensile Modulus of CFRP	6.07	9.08	0.00					

In essence, it assisted in identifying whether the regression line was the best-suited curve to illustrate the link between the sample datasets of two correlated parameters. The null hypothesis, denoted as Ro = 0, states that there is no relationship between the two factors analyzed through ANOVA. The ANOVA model produced two outcomes: an F-statistic, which shows the extent to which the regression formula properly fits the dataset, and another statistic that reflects the significance level of the F-test. If the latter statistic was less than 0.05 at a 95% confidence threshold, the null hypothesis of Ro = 0 was rejected. This demonstrates an association between axial capacity and the target predictor variable, which may be expressed through either a linear or non-linear formula with 95% reliability. Otherwise, it was assumed that the relationship could not be explained as a regression model. Since the F-statistics were less than 0.05, the null hypothesis was dismissed, confirming that the model is valid.

The t-test was employed to evaluate the statistical relevance of the variables in each model, with a 95% confidence threshold. By considering the degrees of freedom linked with each parameter, a t-statistic derived from the experimental results can be compared to a critical value in reference tables. If the calculated t-statistic surpasses the tabled critical value, it implies that the parameter is statistically meaningful at a 95% confidence threshold, with a significance level below 0.05. Thus, the parameter is deemed significant to the model. The obtained p-value for the Column height variable is greater than 0.05 (0.516), suggesting that column height exerts only a minimal effect on axial capacity after the rehabilitation of a fire-damaged column using CFRP.

The Durbin–Watson test was performed to check the degree of multicollinearity. Ideally, Durbin–Watson results should lie between 1.5 and 2.5. The Durbin–Watson value calculated for this model is 2.452, which satisfies this condition. Therefore, this model is not affected by any issues connected to multicollinearity. Fig.4 displays the axial capacity values estimated by the regression model, in comparison with the values observed in experimental tests.

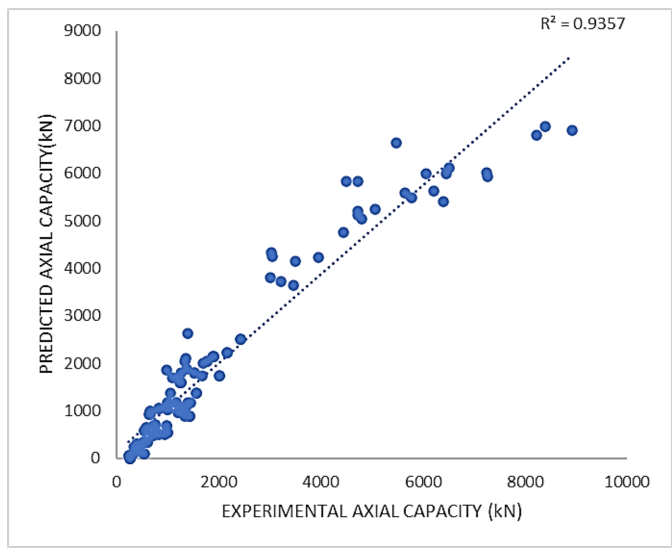

Fig. 4. Comparison of predicted and observed axial capacity for Regression Model

In every instance, the data points are evenly distributed around the r = 1 line, indicating that the models are both plausible and dependable for real-world use. The regression analysis reveals a significant connection between the calculated and anticipated values, as evidenced by the correlation factor (R) of 0.9357. This regression model can be used to forecast the axial capacity of a fire-damaged, repaired concrete column constrained by CFRP.

4.2 Analysis of DNN Models:

In this study, the pursuit of the most accurate and optimal DNN model involved the development of seven distinct DNN models. Among these models, the selection criteria prioritized the identification of the model with the lowest values of RMSE, MSE, and MAE, while also considering the highest correlation factor (R). Initially, single-hidden-layer models were explored, with the number of neurons ranging from 6 to 12. Among these, the model with 10 neurons in the first hidden layer demonstrated the highest correlation factor (R). Subsequently, for models featuring 10 neurons in the first hidden layer, a second hidden layer was introduced, with the number of neurons varying from 8 to 12. Among these two-layered models, it was observed that DNN6-10-10, characterized by 10 neurons in both the first and second hidden layers, exhibited the highest correlation factor (R) and the lowest values of RMSE, MSE, and MAE.

Fig. 5 illustrates the correlation factors of various models, depicting four correlation factor values for each model: training correlation factor, validation R value, testing R value, and overall correlation factor of the model. It is discerned that MD 1-6-00 exhibits the lowest R value for training, at 0.97689, whereas MD 6-10-10 demonstrates the highest R value for training, standing at 0.99926. In contrast, MD 1-6-00 displays the lowest R value for validation, with a magnitude of 0.98256, while MD 6-10-10 boasts the highest R value for validation at 0.99805. Additionally, MD 8-10-08 registers the lowest R value for testing, at 0.97191, whereas MD 6-10-10 secures the highest R value for testing, with a value of 0.99748. Overall, it is evident that MD 6-10-10 boasts the highest overall correlation factor compared to all other models, standing at 0.99852. Conversely, MD 1-6-00 holds the lowest overall correlation factor value, at 0.97937.

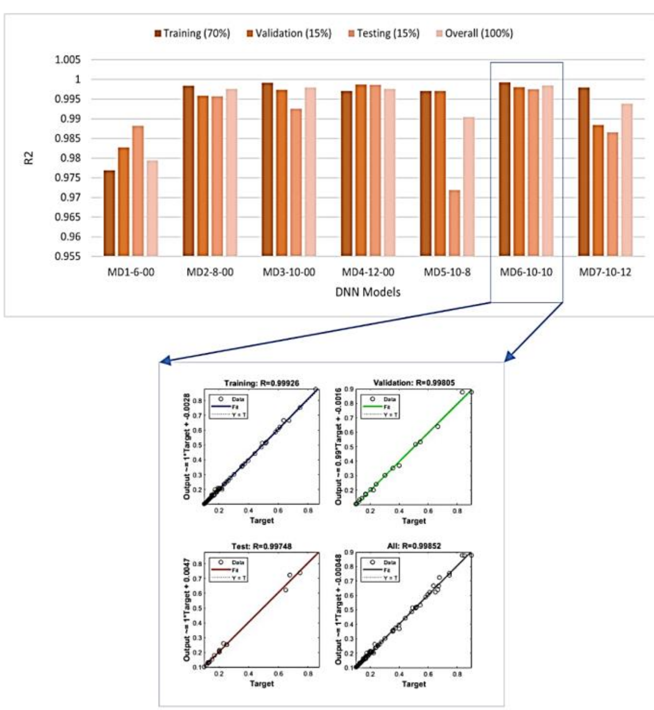

Fig. 5. Training, Validation, Testing and Overall Correlation Factor for DNN Models and optimized MD 6-10-10

In Fig. 5, the correlation factor (R) values of Training, Validation, Testing, and the overall R value for MD 6-10-10 are displayed. The correlation factors for training, validation, testing, and overall are determined to be 0.99926, 0.99805, 0.99748, and 0.99852, respectively. While similar graphs were generated for all other models using MATLAB, MD 6-10-10 is highlighted here due to its proven optimality. The visual representation of R values for MD 6-10-10 indicates a close alignment of the data distribution with the mean line, suggesting strong predictive performance.

4.3 Essential Traits of the Perfect Model:

MD 6-10-10 stands out as the most optimal model, characterized by the highest overall correlation factor (R) of 0.99852 and the lowest values of RMSE, MSE, and MAE. MD 6-10-10 is a double-hidden layered neural model, featuring 10 neurons in the first hidden layer and an additional 10 neurons in the second hidden layer. The general architecture of MD 6-10-10 is depicted in Fig. 6.

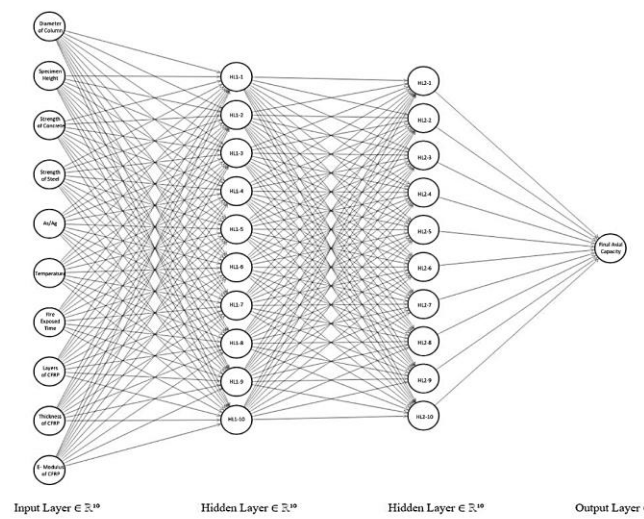

Fig. 6. Architecture of MD 6-10-10

V. Results And Discussion

It is crucial to visually assess the predictive behavior of the model in comparison to the original experimental data collected. Fig. 7 depicts the variation of the predicted axial load capacity by the MD 6-10-10 model and the regression Model relative to the axial load capacity obtained from prior experimental investigations. The analysis reveals that the model's predictions closely align with the original values documented in the literature. Subsequent sections will delve into a more detailed examination of these findings.

Fig. 8 shows the overall correlation factor (R), RMSE, MSE, and MAE of all eight models developed in the present investigation. From Fig. 8, it is clear that with MD6-10-10 exhibiting the highest overall correlation factor of 0.99852, the Figure also displays the Root Mean Square Error (RMSE) of all models, where MD6-10-10 shows the lowest overall RMSE value of 0.0580, and MD1-6-00 has the highest RMSE value among all other models at 0.415. The Mean Square Error (MSE) of all models is presented, with MD6-10-10 once again having the lowest overall MSE value of 0.00337, and MD1-6-00 exhibiting the highest MSE value of 0.1726.

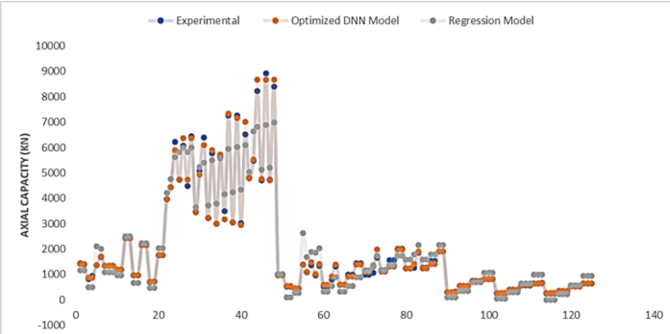

Fig. 7. Comparison between MD 6-10-10 And regression Model predictions and Data collected from Literature review

Similarly, MD6-10-10 has the lowest value of Mean Absolute Error (MAE) among all the models. Finally, the comparison between the optimum DNN Model and the regression Model has also been done.

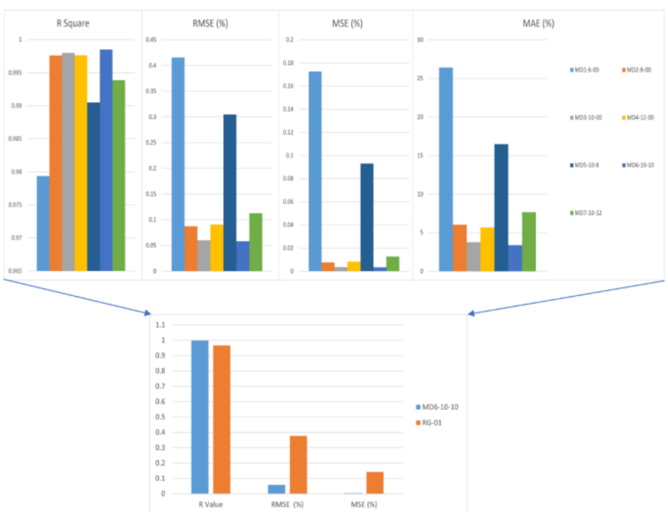

Fig. 8. Statistics of Errors in prediction of axial capacity by proposed models

5.1 *Assessing Prediction Capabilities of Regression and DNN Models*

Table IV shows percentage errors between test results and predictions of the Deep Neural Network (DNN) model and the regression model in the selected studies [5, 65–67]. The table gives an overview of prediction accuracy, outlining the strengths and weaknesses of each model in approximating the axial capacity of fire-damaged concrete columns repaired with Carbon Fiber Reinforced Polymer (CFRP). The percentage error of each experimental value was calculated between the value and the corresponding predictions of both approaches as a direct reflection of model performance.

The comparison of four studies—Yaqub et al. (2010), Hussain et al. (2022), Jia Xu et al. (2022), and Al Nimry et al. (2016)—yields useful data regarding predictive performances of the two models. In Yaqub et al. (2010), the DNN model outperformed the regression model across the board with lower percentage errors. Similar outcomes were observed in research conducted by Hussain et al. (2022) and Jia Xu et al. (2022), where experimental values were better followed by DNN predictions. Again, comparison with Al Nimry et al. (2016) again validated the improved performance of the DNN model over regression analysis.

Despite variations in experimental conditions between the selected studies, the DNN approach consistently yielded more precise results. This proves its robustness and adaptability in predicting the axial capacity of fire-damaged, CFRP-repaired concrete columns under different conditions. Overall, these findings emphasize the potential of advanced machine learning methods namely DNNs in structural engineering. By representing complex relationships in the data, DNN models create more precise predictions, which can allow for better decision-making and aid design methods for fire-damaged structural members.

TABLE IV. ERRORS BETWEEN PREDICTED AND EXPERIMENTAL VALUES OF BOTH DNN AND REGRESSION MODEL

Experimental Value	Predicted Value by NN model	Predicted Value by Regression Model	NN Model Error (%)	Regression Model Error (%)
Comparison With Experimental Study by Yaqub et al.,2010 [5]				
1439	1422.26	1172.92	1.16	18.49
1397	1422.26	1172.92	1.81	16.04
826	880.66	497.74	6.62	39.74
946	880.66	497.74	6.91	47.39
1356	1358.32	2109.72	0.17	55.58
1701	1707.92	2003.64	0.41	17.79
Comparison With Experimental Study by Xu et al.,2022 [66]				
Experimental Value	**Predicted Value by NN model**	**Predicted Value by Regression Model**	**NN Model Error (%)**	**Regression Model Error (%)**
3957	3959.50	4226.29	0.06	6.81
4438	4436.91	4751.41	0.02	7.06
6213	5912.24	5626.59	4.84	9.44
4727	4728.44	5829.30	0.03	23.32
6068	6384.10	6006.28	5.21	1.02
4499	4728.44	5829.30	5.10	29.57
Comparison With Experimental Study by Hussain et al.,2022 [65]				
Experimental Value	**Predicted Value by NN model**	**Predicted Value by Regression Model**	**NN Model Error (%)**	**Regression Model Error (%)**
1353	1351.50	1083.31	0.11	19.93
1351	1351.50	1083.31	0.04	19.81
1355	1351.50	1083.31	0.26	20.05
1196	1200.95	966.94	0.41	19.15
1198	1200.95	966.94	0.25	19.29
2431	2428.68	2518.26	0.10	3.59
Comparison With Experimental Study by Al-Nimry et al.,2016 [67]				
Experimental Value	**Predicted Value by NN model**	**Predicted Value by Regression Model**	**NN Model Error (%)**	**Regression Model Error (%)**
988	983.42	1028.18	0.46	4.07
990	983.42	1028.18	0.66	3.86
534	542.11	103.13	1.52	80.69
536	542.11	103.13	1.14	80.76
457	449.45	269.71	1.65	40.98
459	449.45	269.71	2.08	41.24

Furthermore, the comprehensive examination of the deep neural network (DNN) and regression models in various research highlights the wider range of uses and the higher performance of the DNN.

DNN model utilizes advanced machine learning techniques, that is, Multilayer Feedforward Neural Networks (MLFNNs), to effectively learn from data and tune its predictions for different experimental conditions. This leads to more robust and accurate results. Generally, the analyses made in the paper highlight the relevance of adding the latest machine learning techniques, that is, deep neural network (DNN) models, to the field of structural engineering research and application. These techniques offer a possible means of enhancing the accuracy of prediction and aiding smart decision-making in structural system design and structural system assessment. Figure 9 shows the graphical Representation of the prediction by the DNN and the prediction by the regression model and the comparison with experimental result.

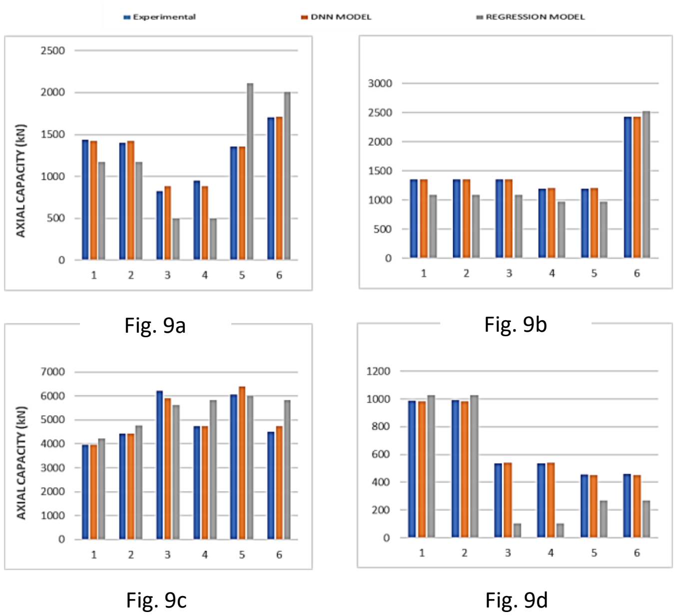

Fig. 9. DNN and Regression Model Prediction Comparison with Experimental Studies by (a) Yaqub et al.,2010 [5] (b) Hussain et al.,2022 [65] (c) Xu et al.,2022 [66] (d) Al-Nimry et al.,2016 [67]

5.2 Analysis Of Effect Of Predictors On Final Axial Capacity

Fig.10 describes the effect of both fire temperature and duration of fire on the axial capacity of circular columns rehabilitated with Carbon Fiber Reinforced Polymer (CFRP) following fire damage. There is a definite reduction in the axial capacity with the increase in exposure time and fire temperature, as the trend suggests. This is consistent with the expected performance of structures that have been damaged by fires. Long-duration heating deteriorates strength and stability as the structural members increasingly lose their ability to sustain axial loads. Furthermore, rising fire temperatures increase this deterioration further lowering the column's integrity. Thus, the lowest axial capacity is observed when temperature and duration of fire are at their highest values. This trend further advocates for the importance of incorporating fire effects into structural element design and assessment, particularly in CFRP-strengthened concrete columns. An understanding of column behavior under fire exposure is essential to ensure they are safe and trustworthy in real-world conditions. Lastly, results from Fig. 10 can be employed towards the development of design considerations and guidelines for improving structural system fire resistance as well as overall performance under fire-exposed environments.

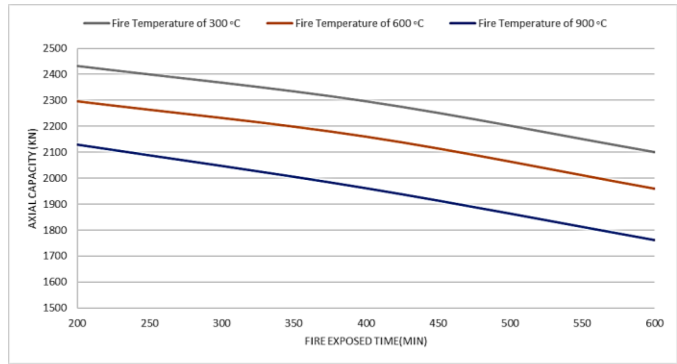

Fig. 10. Effect of Fire Exposed Time and Fire Temperature on Axial strength of Fire damaged, CFRP repaired Circular Columns

Fig. 11 illustrates the correlation between the quantity of Carbon Fiber Reinforced Polymer (CFRP) layers and the fire temperature on the axial capacity of fire-damaged circular columns that have been restored using CFRP. The illustrated pattern demonstrates that the axial capacity rises as the number of CFRP layers increases, whereas it decreases as the fire temperature rises. The increase in axial capacity resulting from the addition of more CFRP layers aligns with the strengthening impact of CFRP materials on columns damaged by fire. Extra layers of CFRP strengthen the structural reinforcement, hence boosting the overall load-carrying capability of the columns. This event highlights the efficacy of CFRP as a reinforcement material in mitigating the adverse effects of fire-induced damage on structural integrity.

On the other hand, the reduction in the ability to bear weight along the axis as fire temperatures increase emphasizes the harmful effect of high thermal conditions on the strength and stability of the structure. As the temperature of the fire rises, the mechanical characteristics of both the concrete and CFRP materials deteriorate, resulting in a decrease in the structural integrity. Therefore, the axial capacity is at its lowest when there are no CFRP layers and the fire temperature is at its highest, indicating the most extreme conditions for structural performance. Figure 11's insights highlight the importance of considering the quantity of CFRP layers and fire temperature when designing and evaluating fire-damaged structures repaired with CFRP. Engineers can enhance the fire resistance and resilience of structural systems by understanding the interaction between these components. This understanding allows them to optimize strengthening measures, ensuring the safety and longevity of the systems in fire-prone areas.

Fig. 12 illustrates an examination of how the quantity of Carbon Fiber Reinforced Polymer (CFRP) layers and the temperature of fire exposure affect the axial capacity of circular columns that have been restored with CFRP after being damaged by fire. The trends shown indicate a direct relationship between the number of CFRP layers and axial capacity, while a reverse relationship is detected between fire exposure time and axial capacity.

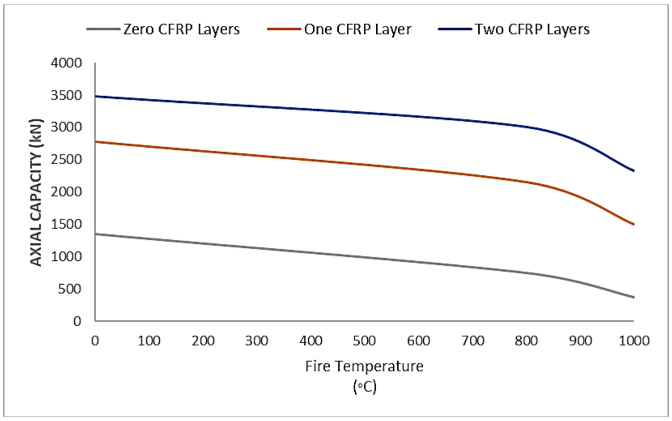

Fig. 11. Effect of No of CFRP layers and Fire Temperature on Axial strength of Fire damaged, CFRP repaired Circular Columns

Moreover, Fig. 12 clearly illustrates that the highest axial capacity is achieved when two layers of CFRP are used, with no fire exposure. This discovery highlights the synergistic effect of CFRP reinforcement and the absence of fire-induced damage, resulting in exceptional structural performance. The significance of Fig. 12 lies in its ability to emphasize the necessity of thoroughly evaluating the quantity of CFRP layers and the duration of fire exposure when designing and restoring structures damaged by fire. Engineers can enhance the fire resistance and resilience of structural systems in fire-prone situations by deliberately optimizing these parameters. This ensures the safety and longevity of the systems.

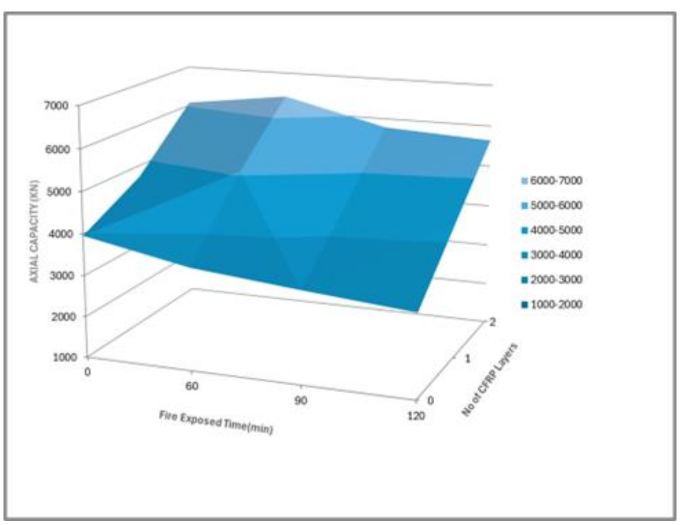

Fig. 12. Effect of No of CFRP layers and Fire Exposed Temperature on Axial strength of Fire damaged, CFRP repaired Circular Columns

VI. Conclusion

The performance assessment of the tested Artificial Neural Network (ANN) models in forecasting the axial capacity of fire-damaged columns repaired with Carbon Fiber Reinforced Polymer (CFRP) has proven their superiority over Multiple Regression Analysis (MRA), as evidenced by comparisons of various performance indices. The results highlight the efficacy of ANN models in accurately forecasting axial capacity, particularly when compared to empirical data from multiple studies. Nevertheless, it is acknowledged that the artificial neural network (ANN) method would be advantageous if a more extensive and varied training set were created to augment its predictive skills further. After conducting a thorough analysis using ANN and MRA techniques the following conclusion can be drawn:

- MD 6-10-10 stands out as the most optimal model, characterized by the highest overall correlation factor (R) of 0.99852 and the lowest values of RMSE, MSE, and MAE with RMSE (%) = 0.058, MSE (%) =0.0033 and MAE (%) =3.38. MD 6-10-10 is a double hidden layered neural model, featuring 10 neurons in the first hidden layer and an additional 10 neurons in the second hidden layer.
- The ANN models, especially MD6-10-10, accurately predicted the axial capacity when compared to Experimental data from various studies. This highlights the potential of ANN models in aiding the design process for repairing fire-damaged Circular concrete columns with CFRP composites.
- During the comparative study of Predicted Results with the original experimental studies conducted in the literature. It is established that the proposed DNN model gives accurate results with an absolute error as low as 0.02%. Hence the developed model can be used during the design process of repairing fire damaged Circular concrete columns with CFRP composites.
- While MRA is simple and does not require sophisticated software, it may not accurately represent nonlinear relationships in the data. ANN models, on the other hand, are highly effective in capturing complex and nonlinear functional connections. Despite requiring sophisticated computations and extensive training data, ANN models offer superior predictive accuracy and flexibility with low error percentage of 0.02%
- The predictions indicated that the number of CFRP layers significantly influences the restored axial strength of fire-damaged columns. Two Number of CFRP layers result in up to 83% increase in axial strength.
- The duration and temperature of the fire are critical factors affecting the repaired axial strength. Higher fire duration and temperature result in lower repaired axial strength.

These findings underscore the dependability and suitability of the developed ANN models, particularly the MD6-10-10 model, in assisting the design process of restoring fire-damaged columns using CFRP composites. The insights gained from this study provide valuable guidance for engineers to enhance repair strategies and ensure the safety and resilience of structures in fire-prone environments.

VII. REFERENCES:

[1] Bisby, L.A., A. Dent, and M.F.J.A.S.J. Green, Comparison of confinement models for FRP wrapped concrete. 2005. 102(1): p. 62-72.

[2] De Lorenzis, L. and R.J.J.o.C.f.C. Tepfers, Comparative study of models on confinement of concrete cylinders with fiber-reinforced polymer composites. 2003. 7(3): p. 219-237.

[3] Bisby, L., V. Kodur, and M.J.A.S.J. Green, Fire endurance of fiber-reinforced polymer-confined concrete. 2005. 102(6): p. 883-891.

[4] Chowdhury, E., et al. Fire behaviour of FRP wrapped square reinforced concrete columns. in Third International Conference on Durability and Field Applications of Fibre Reinforced Polymer (FRP) Composites for Construction (CDCC-07), Quebec City, Canada. 2007.

[5] Yaqub, M., C.J.C. Bailey, and B. Materials, Repair of fire damaged circular reinforced concrete columns with FRP composites. 2011. 25(1): p. 359-370.

[6] Himick, M. and S. Bouriaux, Securitized insurance risk: strategic opportunities for insurers and investors. 1998: Global Professional Publishi.

[7] Akhtar, Ali, Shahzad Saleem, Muhammad Salman, Muhammad Noman, Mohammad Zulqarnain, and Tidarut Jirawattanasomkul. "Performance of square masonry columns retrofitted with NSM steel and GFRP reinforcement under axial compression." *Construction and Building Materials* 458 (2025): 139534.

[8] M. . Salman, M. . Arshad, M. . Noman, S. . Ullah Khan, A. . Ahmed, and M. . Hussain, “Analyzing Transit Stop Service Areas Using Geographic Information Systems (GIS): A Case Study of UET Taxila”, *JoCEF*, vol. 6, no. 02, pp. 97-102, Sep. 2025..

[9] Chinthapalli, H.K. and A.J.J.o.S.E. Agarwal, Effect of confining reinforcement on fire behavior of reinforced concrete columns: experimental and numerical study. 2020. 146(6): p. 04020084.

[10] Ehsana, M.A., et al., Effectiveness of prolonged air-recuring on strength of fire damaged RC columns. 2019. 5(10): p. 2207-2220.

[11] Usman, M., et al., Restorability of strength and stiffness of fire damaged concrete using various composite confinement techniques. 2021. 272: p. 121984.

[12] Noman, Muhammad, Muhammad Salman, Afaq Ahmed, Muzammal Hussain, Ali Akhtar, and Mohammad Zulqarnain. "Repair of Fire-Damaged Circular and Square Columns Using CFRP Composites: A Comprehensive Review." *Journal OF Civil Engineering* 6, no. 02 (2025): 82-96.

[13] Toutanji, H., et al., Behavior of large-scale rectangular columns confined with FRP composites. 2010. 14(1): p. 62-71.

[14] Issa, M.A., R.Z. Alrousan, and M.A.J.J.o.C.f.C. Issa, Experimental and parametric study of circular short columns confined with CFRP composites. 2009. 13(2): p. 135-147.

[15] Benzaid, R., et al., Behaviour of square concrete column confined with GFRP composite warp. 2008. 14(2): p. 115-120.

[16] Kumutha, R., et al., Behaviour of reinforced concrete rectangular columns strengthened using GFRP. 2007. 29(8): p. 609-615.

[17] Kumutha, R., M.J.J.o.r.p. Palanichamy, and composites, Investigation of reinforced concrete columns confined using glass fiber-reinforced polymers. 2006. 25(16): p. 1669-1678.

[18] Marques, S.P.C., et al., Model for analysis of short columns of concrete confined by fiber-reinforced polymer. 2004. 8(4): p. 332-340.

[19] Chaallal, O., M. Shahawy, and M.J.J.o.C.f.C. Hassan, Performance of axially loaded short rectangular columns strengthened with carbon fiber-reinforced polymer wrapping. 2003. 7(3): p. 200-208.

[20] Demers, M. and K.W.J.C.J.o.C.E. Neale, Confinement of reinforced concrete columns with fibre-reinforced composite sheets-an experimental study. 1999. 26(2): p. 226-241.

[21] Yaqub, M., et al., Axial capacity of post-heated square columns wrapped with FRP composites. 2011. 33(6): p. 694-701.

[22] Moghtadernejad, N., et al. Repair of post-heated short rectangular reinforced concrete columns with FRP jackets. in Structures. 2021. Elsevier.

[23] Al-Nimry, H., et al., Effectiveness of advanced composites in repairing heat-damaged RC columns. 2013. 46: p. 1843-1860.

[24] Chowdhury, E., et al., Residual behavior of fire-exposed reinforced concrete beams prestrengthened in flexure with fiber-reinforced polymer sheets. 2008. 12(1): p. 61-68.

[25] Chowdhury, E.U., et al., Investigation of insulated FRP-wrapped reinforced concrete columns in fire. 2007. 42(6-7): p. 452-460.

[26] Green, M.F., et al., FRP confined concrete columns: Behaviour under extreme conditions. 2006. 28(10): p. 928-937.

[27] Kodur, V.K., L.A. Bisby, and M.F.J.F.s.j. Green, Experimental evaluation of the fire behaviour of insulated fibre-reinforced-polymer-strengthened reinforced concrete columns. 2006. 41(7): p. 547-557.

[28] Williams, B., et al., Fire insulation schemes for FRP-strengthened concrete slabs. 2006. 37(8): p. 1151-1160.

[29] Kodur, V., L. Bisby, and M.F. Green. Fire endurance of FRP-strengthened reinforced concrete columns. in Proceedings of the fourth international conference on concrete under severe conditions, Seoul, Korea. 2004.

[30] Fletcher, I.A., et al., Behaviour of concrete structures in fire. 2007. 11(2): p. 37-52.

[31] Industry, C.J.T.C.S., Assessment, design and repair of fire-damaged concrete structures. 2008.

[32] Buchanan, A.H. and A.K. Abu, Structural design for fire safety. 2017: John Wiley & Sons.

[33] Takemura, H.J.S.E.J., JSCE, A, Effect of hysteresis on ductility capacity of reinforced concrete bridge piers. 1997. 43: p. 849-848.

[34] Hoshikuma, J., et al., Stress-strain model for confined reinforced concrete in bridge piers. 1997. 123(5): p. 624-633.

[35] Kawashima, K., G. Shoji, and Y.J.J.o.S.E.A. Sakakibara, A cyclic loading test for clarifying the plastic hinge length of reinforced concrete piers. 2000. 46: p. 767-776.

[36] Saeed, H.Z., et al., Experimental and finite element investigation of strengthened LSC bridge piers under Quasi-Static Cyclic Load Test. 2015. 131: p. 556-564.

[37] Khan, Q.-U.-Z., et al., Seismic evaluation of repaired and retrofitted circular bridge piers of low-strength concrete. 2015. 40: p. 3057-3066.

[38] Khan, Q.u.Z., et al. Energy dissipation characteristics of retrofitted damaged low-strength concrete bridge pier. in Proceedings of the Institution of Civil Engineers-Bridge Engineering. 2021. Thomas Telford Ltd.

[39] Cascardi, A., F. Micelli, and M.A.J.E.S. Aiello, An Artificial Neural Networks model for the prediction of the compressive strength of FRP-confined concrete circular columns. 2017. 140: p. 199-208.

[40] Naderpour, H., et al., Innovative models for prediction of compressive strength of FRP-confined circular reinforced concrete columns using soft computing methods. 2019. 215: p. 69-84.

[41] Stamopoulos, A., K. Tserpes, and A.J.C.S. Dentsoras, Quality assessment of porous CFRP specimens using X-ray Computed Tomography data and Artificial Neural Networks. 2018. 192: p. 327-335.

[42] Le-Nguyen, K., et al., Development of deep neural network model to predict the compressive strength of FRCM confined columns. 2022. 16(10): p. 1213-1232.

[43] Al-Khaleefi, A.M., et al., Prediction of fire resistance of concrete filled tubular steel columns using neural networks. 2002. 37(4): p. 339-352.

[44] Abbas, H., et al., ANN models for prediction of residual strength of HSC after exposure to elevated temperature. 2019. 106: p. 13-28.

[45] Yadollahi, M.M., et al., Estimating of FRP-confined compressive strength of elevated temperature damaged concrete using ANN. 2012. 65: p. 384-393.

[46] Myers, R.H. and R.H. Myers, Classical and modern regression with applications. Vol. 2. 1990: Duxbury press Belmont, CA.

[47] Lawal, B. and H.B. Lawal, Categorical data analysis with SAS and SPSS applications. 2003: Psychology Press.

[48] Cladera, A. and A.J.E.s. Mari, Shear design procedure for reinforced normal and high-strength concrete beams using artificial neural networks. Part II: beams with stirrups. 2004. 26(7): p. 927-936.

[49] Cladera, A. and A.J.E.s. Marí, Shear design procedure for reinforced normal and high-strength concrete beams using artificial neural networks. Part I: beams without stirrups. 2004. 26(7): p. 917-926.

[50] LeCun, Y., Y. Bengio, and G.J.n. Hinton, Deep learning. 2015. 521(7553): p. 436-444.

[51] Bishop, C.M. and N.M. Nasrabadi, Pattern recognition and machine learning. Vol. 4. 2006: Springer.

[52] Rumelhart, D.E., G.E. Hinton, and R.J.J.n. Williams, Learning representations by back-propagating errors. 1986. 323(6088): p. 533-536.

[53] Ruder, S.J.a.p.a., An overview of gradient descent optimization algorithms. 2016.

[54] Svozil, D., et al., Introduction to multi-layer feed-forward neural networks. 1997. 39(1): p. 43-62.

[55] LeCun, Y., et al., Efficient backprop, in Neural networks: Tricks of the trade. 2002, Springer. p. 9-50.

[56] Rojas, R., Neural networks: a systematic introduction. 2013: Springer Science & Business Media.

[57] Wilson, D.R. and T.R.J.N.n. Martinez, The general inefficiency of batch training for gradient descent learning. 2003. 16(10): p. 1429-1451.

[58] Beale, M.H., M.T. Hagan, and H.B.J.U.s.G. Demuth, MathWorks, Neural network toolbox. 2010. 2: p. 77-81.

[59] Koivo, H.N., Basics using MATLAB Neural Network Toolbox.

[60] Ahmad, A., D.M. Cotsovos, and N.D.J.S.A.S. Lagaros, Framework for the development of artificial neural networks for predicting the load carrying capacity of RC members. 2020. 2: p. 1-21.

[61] Özkan, C., F.S.J.P.E. Erbek, and R. Sensing, The comparison of activation functions for multispectral Landsat TM image classification. 2003. 69(11): p. 1225-1234.

[62] Hassoun, M.H., Fundamentals of artificial neural networks. 1995: MIT press.

[63] Glorot, X. and Y. Bengio. Understanding the difficulty of training deep feedforward neural networks. in Proceedings of the thirteenth international conference on artificial intelligence and statistics. 2010. JMLR Workshop and Conference Proceedings.

[64] Al-Kamaki, Y.S., R. Al-Mahaidi, and I.J.C.S. Bennetts, Experimental and numerical study of the behaviour of heat-damaged RC circular columns confined with CFRP fabric. 2015. 133: p. 679-690.

[65] Hussain, I., et al. Finite element modeling and statistical analysis of fire-damaged reinforced concrete columns repaired using smart materials and FRP confinement. in 10th International Conference on FRP Composites in Civil Engineering: Proceedings of CICE 2020/2021 10. 2022. Springer.

[66] Xu, J., Circular Reinforced Concrete Columns Damaged By Fire and Retrofitted With Cfrp and Steel Jacketing. 2022, Syracuse University.

[67] Al-Nimry, H.S., A.M.J.I.J.o.C.S. Ghanem, and Materials, FRP confinement of heat-damaged circular RC columns. 2017. 11: p. 115-133.

[68] Siddiqui, N.A., et al., Experimental investigation of slender circular RC columns strengthened with FRP composites. 2014. 69: p. 323-334.

[69] Benzaid, R. and H.A.J.F.r.p.T.t.a.f.c.r. Mesbah, Circular and square concrete columns externally confined by CFRP composite: experimental investigation and effective strength models. 2013: p. 167-201.

[70] Wang, J., et al., Research and application of an air quality early warning system based on a modified least squares support vector machine and a cloud model. 2017. 14(3): p. 249.